Electronic Supplementary Material (ESI) for Journal of Materials Chemistry C.

Supplementary Information

Expanding the Horizons for Viable Precursors and Liquid Fluxes for the Synthesis of $BaZrS_3$ and Related Compounds

Kiruba Catherine Vincent[*, a], Shubhanshu Agarwal[*, a], Zirui Fan[a], Alison Sofia Mesa Canizales[b], and Rakesh Agrawal[**, a]

[a]Davidson School of Chemical Engineering, Purdue University, West Lafayette, IN 47907(USA)
[b]Chemical and Environmental Engineering, Universidad Nacional de Colombia, Bogota D.C. (Colombia)

*Equal Contribution
**Corresponding author: Dr. Rakesh Agrawal. E-mail: agrawalr@purdue.edu

Ba-Zr-S powder reactions

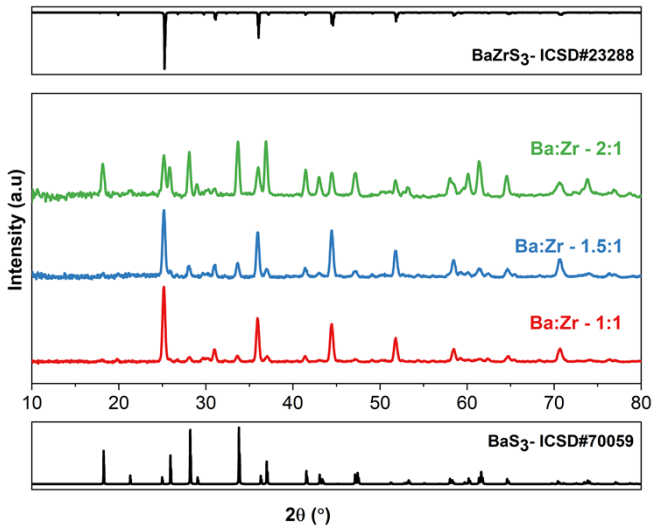

Figure S1. X-ray diffraction pattern of Ba-Zr-S powder synthesized with different Ba:Zr ratios at 575 °C for 12 h with a sulfur pressure of 0.79 atm. BaS and ZrS_2 were used as barium and zirconium precursors, respectively. The X-ray diffraction patterns were collected before rinsing the powders with water as against data in Figure 1.a.

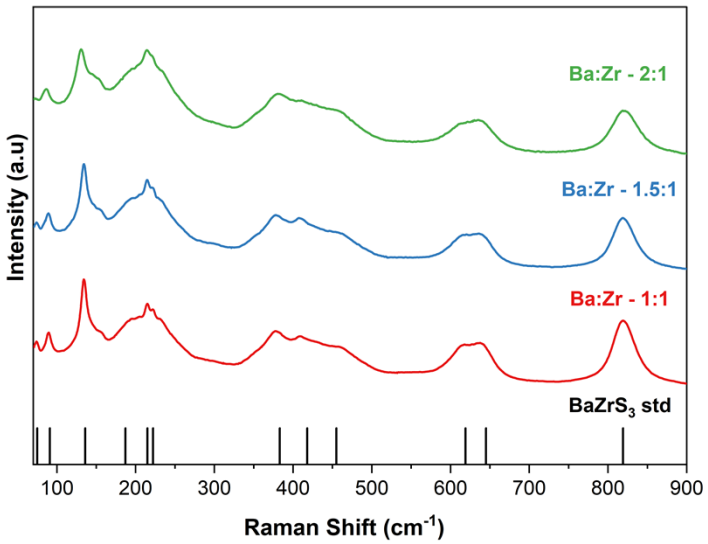

Figure S2. Raman spectra of Ba-Zr-S powder synthesized with different Ba:Zr ratios at 575 °C for 12 h with a sulfur pressure of 0.79 atm. The synthesized powder was washed with water to remove water-soluble impurities (BaS_3). BaS and ZrS_2 were used as barium and zirconium precursors, respectively.

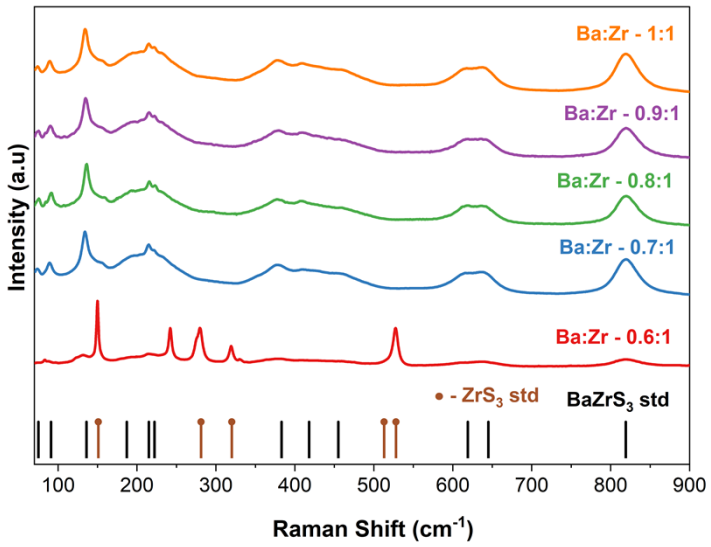

Figure S3. Raman spectra of Ba-Zr-S powder synthesized with different Ba:Zr ratios at 575 °C for 12 h with a sulfur pressure of 0.79 atm. BaS and ZrS_2 were used as barium and zirconium precursors, respectively.

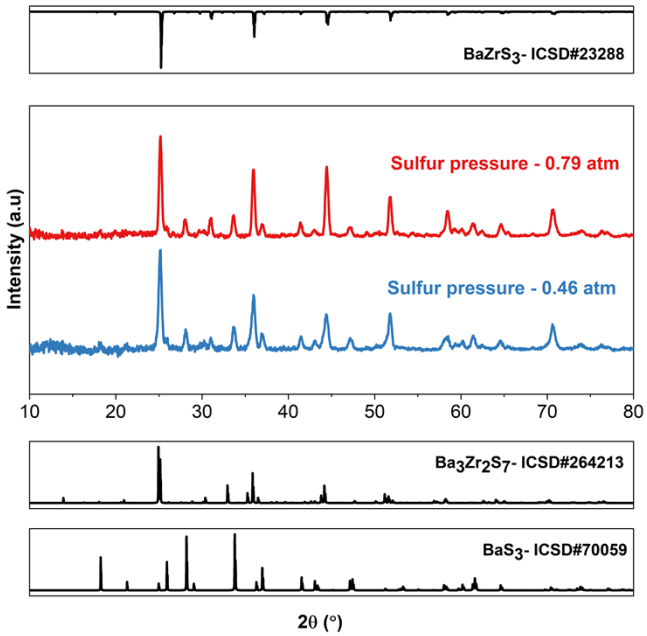

Figure S4. X-ray diffraction pattern of Ba-Zr-S powder synthesized with a Ba:Zr ratio of 1.5:1 and sulfur pressures of 0.79 atm and 0.46 atm, respectively, at 575 °C for 12 h. BaS and ZrS_2 were used as barium and zirconium precursors, respectively.

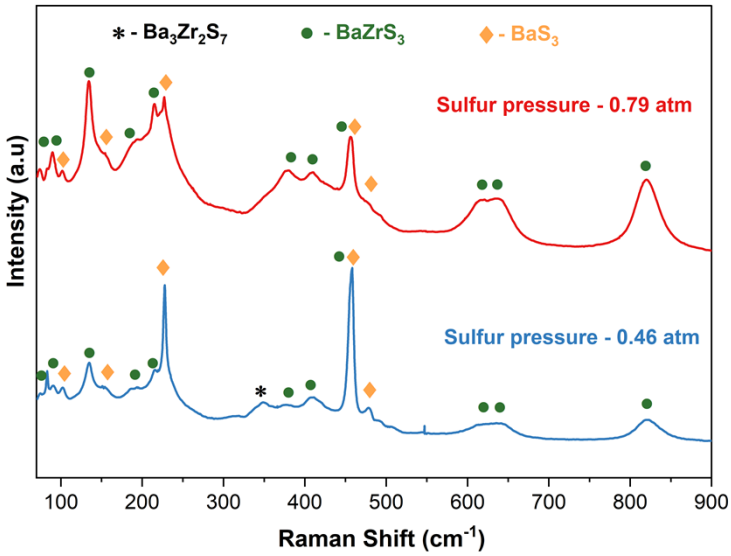

Figure S5. Raman spectra of Ba-Zr-S powder synthesized with a Ba:Zr ratio of 1.5:1 and sulfur pressures of 0.79 atm and 0.46 atm, respectively, at 575 °C for 12 h. BaS and ZrS_2 were used as barium and zirconium precursors, respectively.

Stacked binary metal sulfides

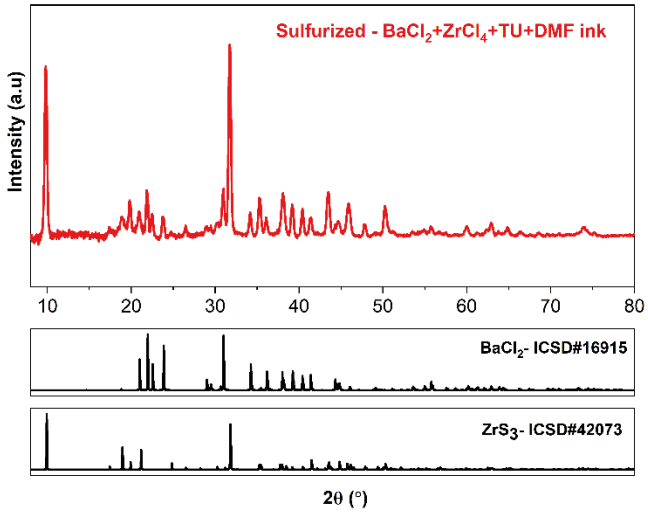

Figure S6. X-ray diffraction analysis confirmed the formation of $BaCl_2$ and ZrS_3 after sulfurizing the as-annealed film obtained from the mixed precursor ink of $BaCl_2$-$ZrCl_4$-thiourea (TU)-dimethyl formamide (DMF). The film underwent sulfurization at 575 °C for 12 h.

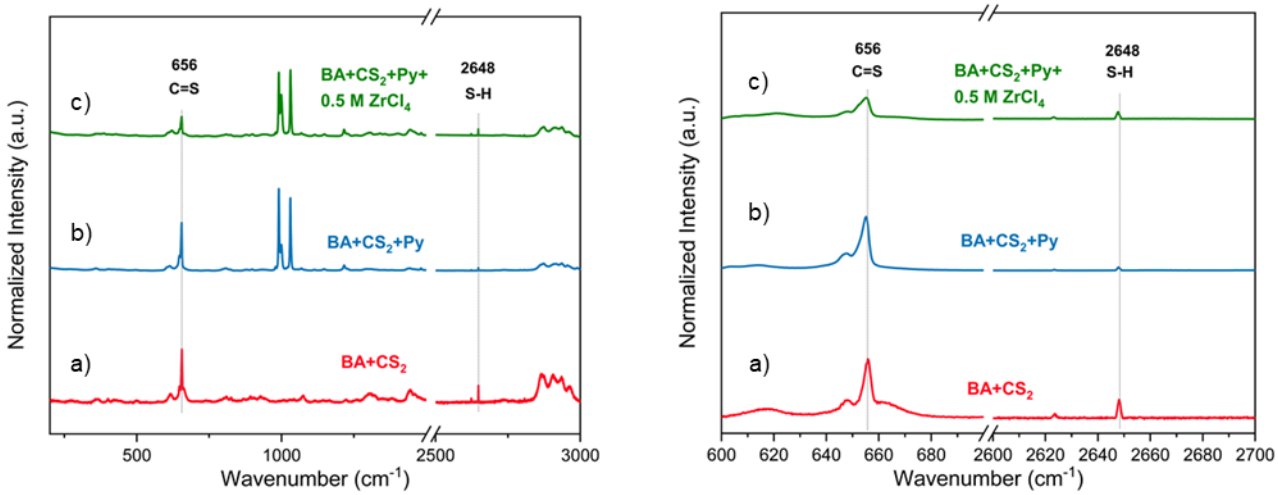

Figure S7. Liquid Raman on a) Butylamine (BA)+CS_2, b) BA+CS_2+Pyridine (Py), and c) BA+CS_2+Py+$ZrCl_4$ (0.5 M). The emergence of a new peak at 2648 cm^{-1} suggests the formation of the dithiocarbamate group. The broadening of the C=S peak at 656 cm^{-1} in (c) indicate metal-sulfur interaction.

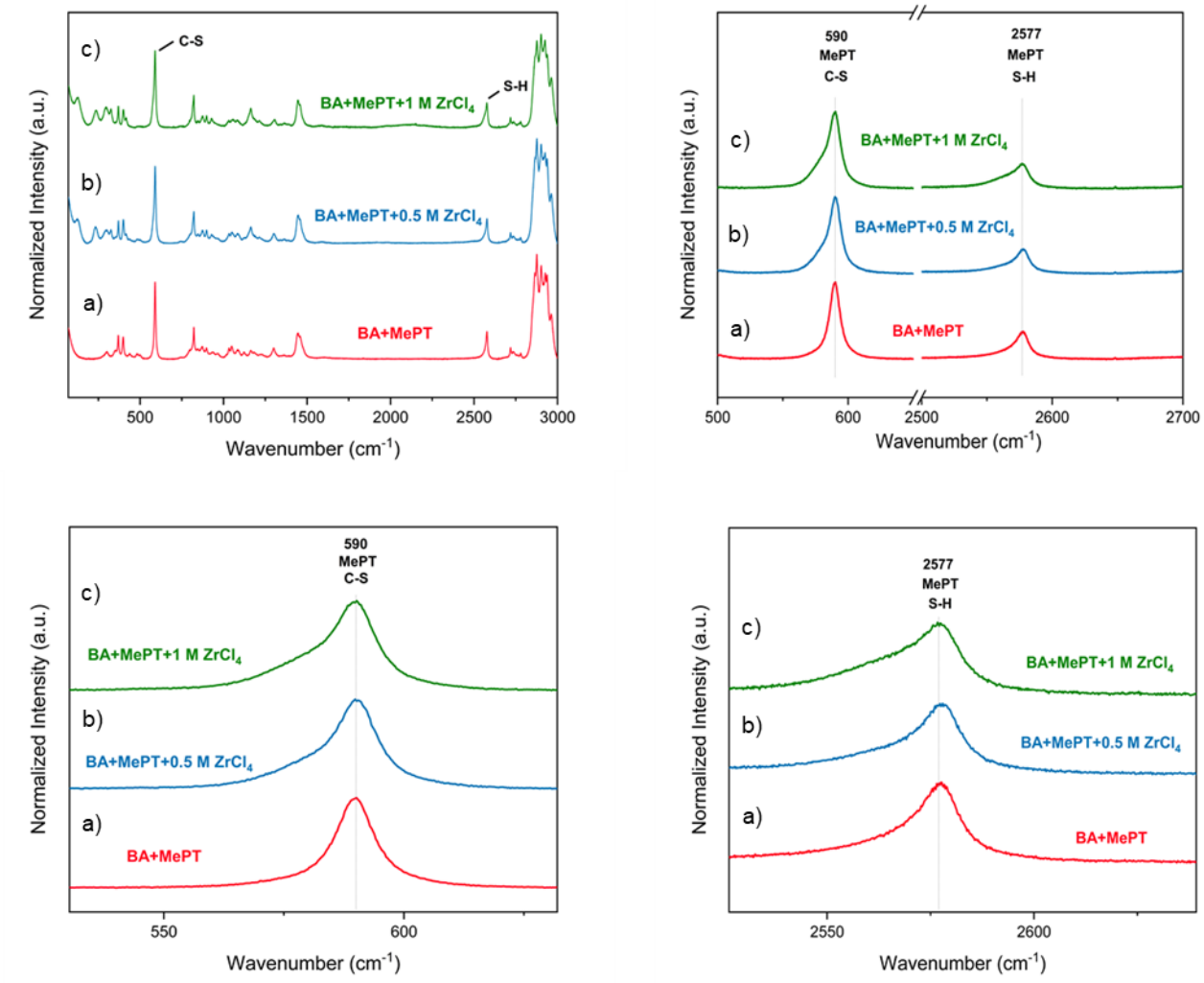

Figure S8. Liquid Raman on Butylamine a) (BA)+2-methyl-2-propanethiol (MePT), b) BA+MePT+$ZrCl_4$ (0.5 M), and c) BA+MePT+$ZrCl_4$ (1 M). The slight broadening and reduction in the ratio of area under peaks of SH to C-S from 0.62 to 0.49 suggests the interaction of metal, sulfur, and thiolate formation. However, insufficient SH peak intensity reduction means the complete substitution of chlorine with thiolate did not occur.

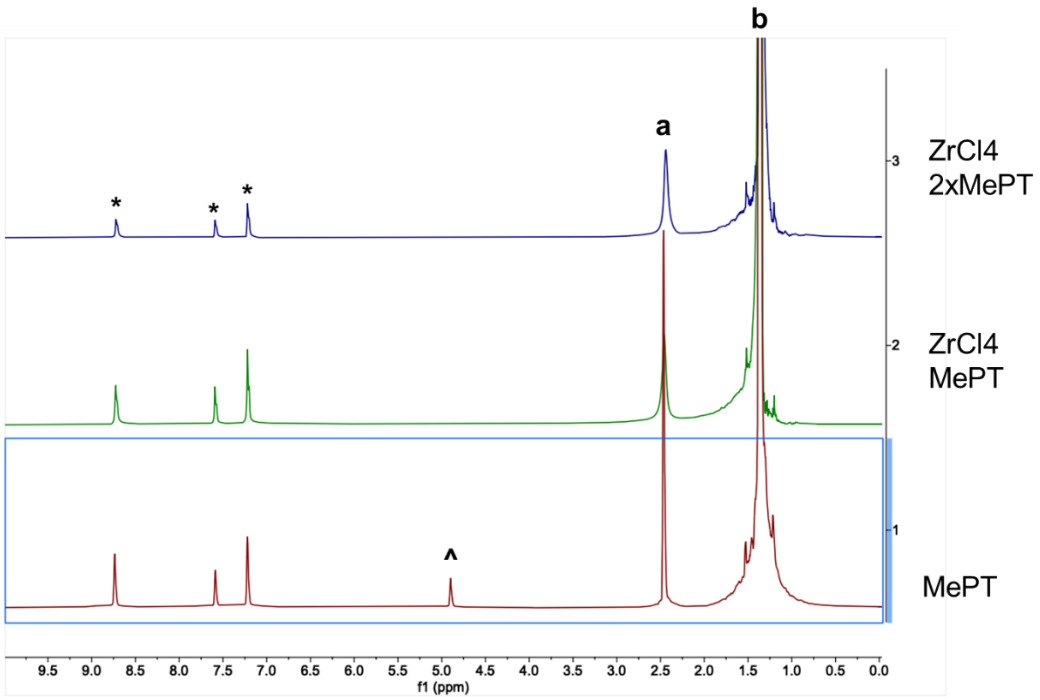

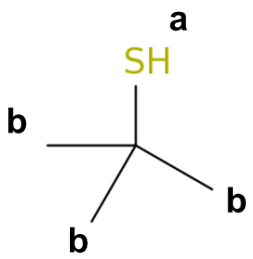

^ water

* d-pyridine

Figure S9. ^{1}H-NMR analysis on only 2-methyl-2-propanethiol (MePT), stoichiometric MePT+$ZrCl_4$, and twice stoichiometric MePT+$ZrCl_4$ in d-pyridine. The slight broadening of the peak for H bound to sulfur suggests the interaction of metal and sulfur and thiolate formation. However, insufficient SH peak intensity reduction means that complete substitution of chlorine with thiolate did not occur.

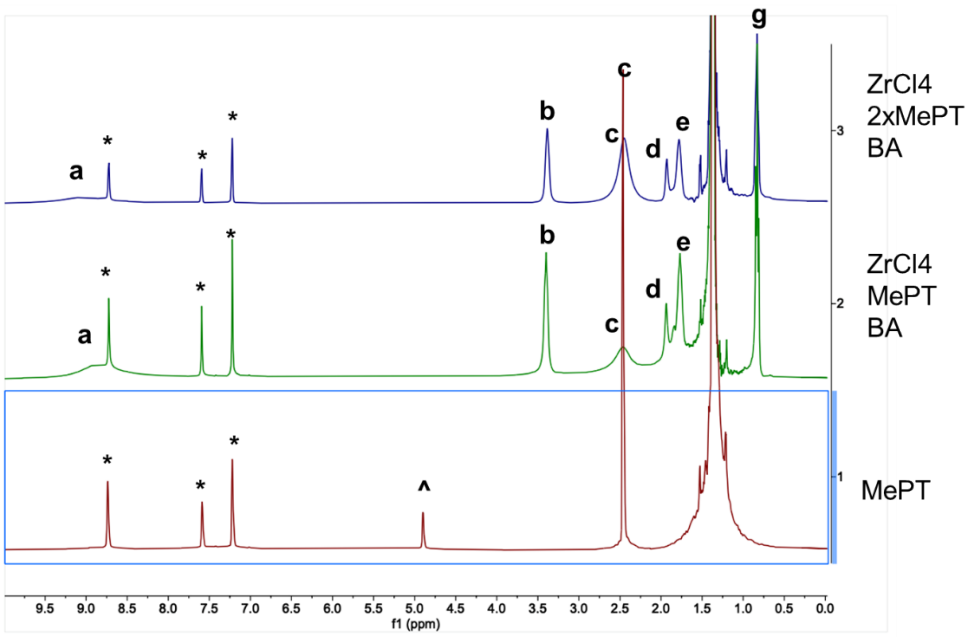

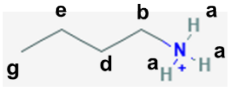

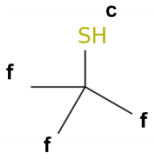

^ water

* d-pyridine

Figure S10. [1]H-NMR analysis on only 2-methyl-2-propanethiol (MePT), stoichiometric MePT+ stoichiometric butylamine (BA)+$ZrCl_4$, and twice stoichiometric MePT+stoichiometric BA+$ZrCl_4$ in d-pyridine. The broadening of the peak for proton bound to sulfur and reduction in the ratio of the peak intensities of proton at a-site to proton at b-site suggests the increased interaction of thiol and Butylamine as such intensity reduction was not observed without Butylamine.

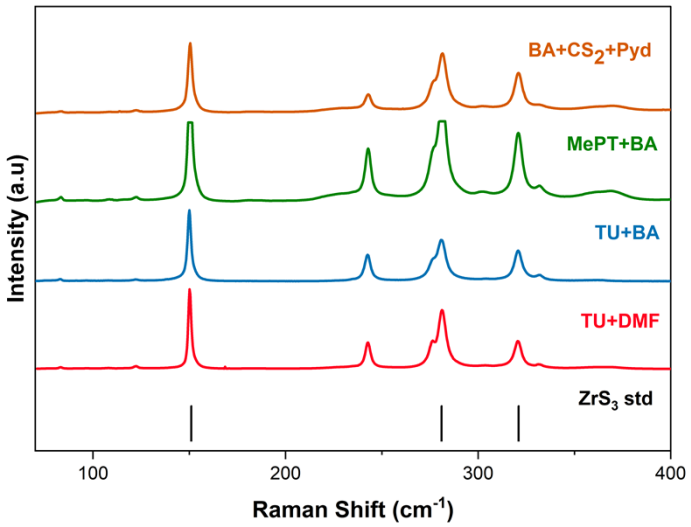

Figure S11. Raman of ZrS_3 film synthesized from 4 different solution chemistries with $ZrCl_4$ metal precursor. The films were sulfurized at 575 °C for 6 h. Reference Raman peaks were identified by Osada et al.[2]

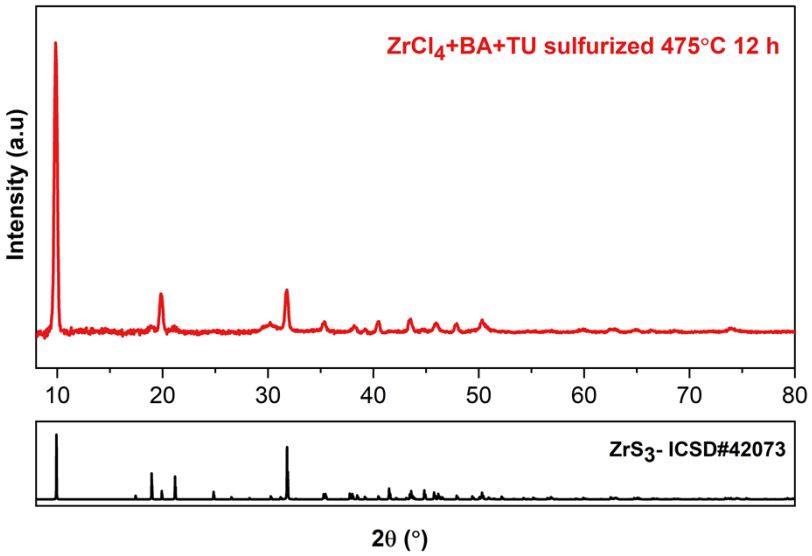

Figure S12. X-ray diffraction pattern of ZrS_3 film synthesized from $ZrCl_4$ precursors. The films were sulfurized at 475 °C for 12 h.

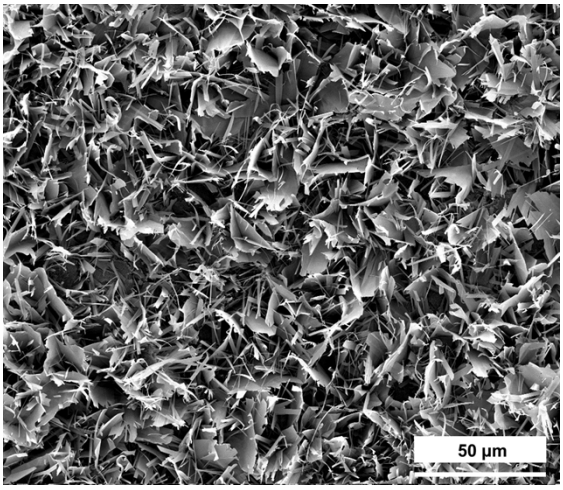

Figure S13. SEM top view of ZrS_3 film synthesized from $ZrCl_4$-2-methyl-2-propanethiol-butylamine solution chemistry. The film was sulfurized at 575 °C for 6 h.

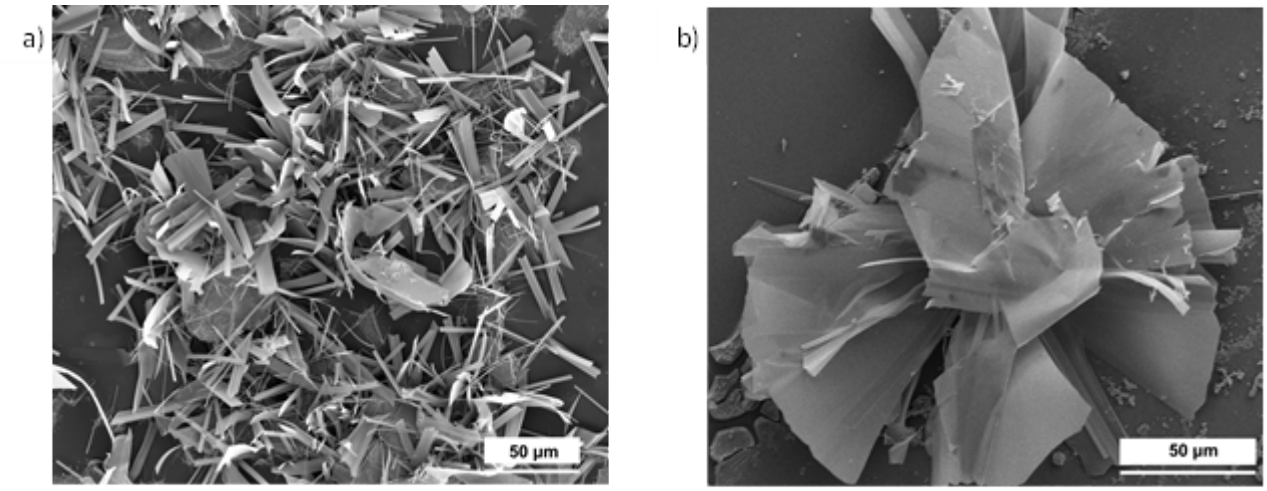

Figure S14. SEM top view of ZrS_3 films synthesized from a) $ZrCl_4$-thiourea-dimethyl formamide solution chemistry and b) $ZrCl_4$-thiourea-butylamine solution chemistry. The films were sulfurized at 575 °C for 6 h.

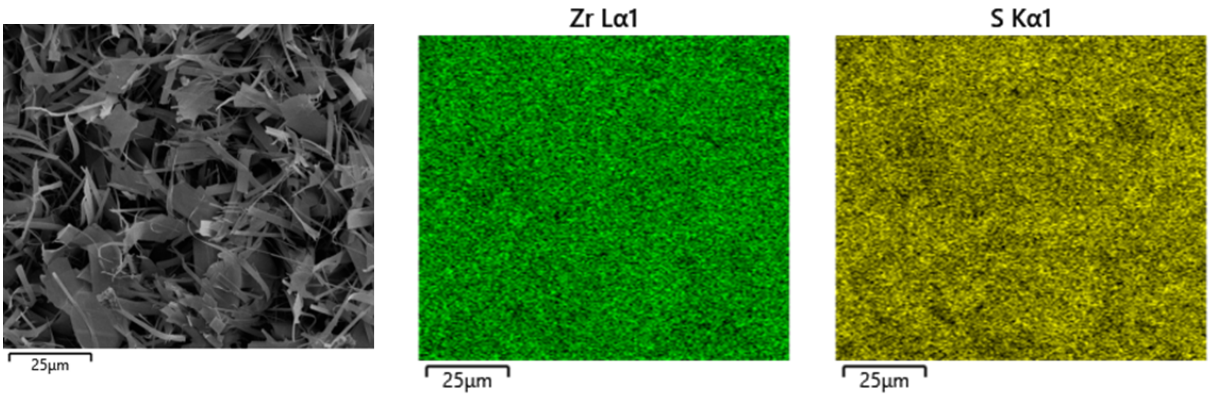

Figure 15. EDX mapping of ZrS_3 film synthesized from $ZrCl_4$-butylamine-CS_2-pyridine solution chemistry confirms only Zr and S in the ZrS_3 grains. The film was sulfurized at 575 °C for 6 h.

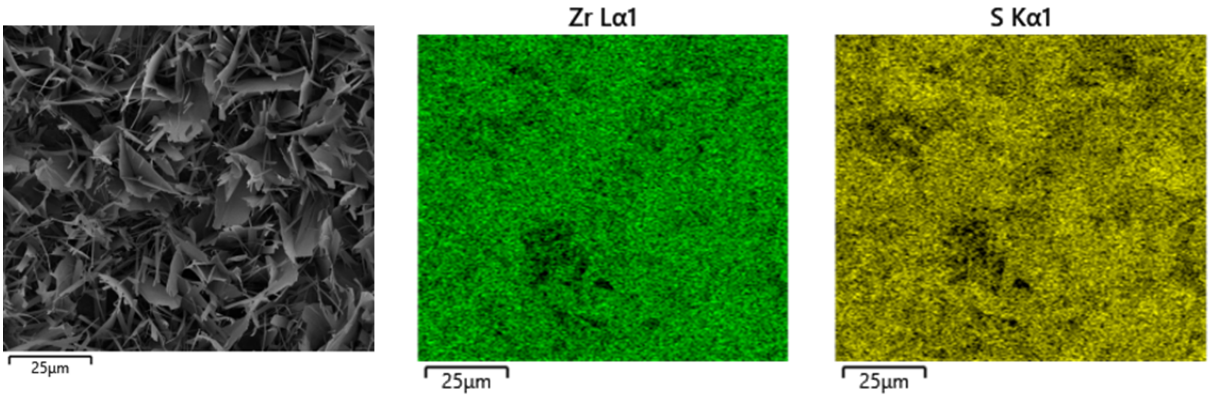

Figure S16. EDX mapping of ZrS_3 film synthesized from $ZrCl_4$-2-methyl-2-propanethiol-butylamine solution chemistry confirms the presence of only Zr and S in the ZrS_3 grains. The film was sulfurized at 575 °C for 6 h.

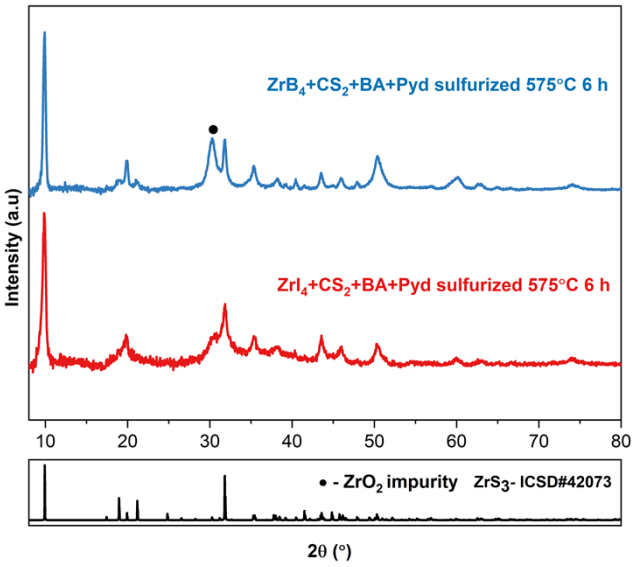

Figure S17. X-ray diffraction pattern of ZrS_3 film synthesized from $ZrBr_4$ and ZrI_4 metal precursors. The films were sulfurized at 575 °C for 6 h.

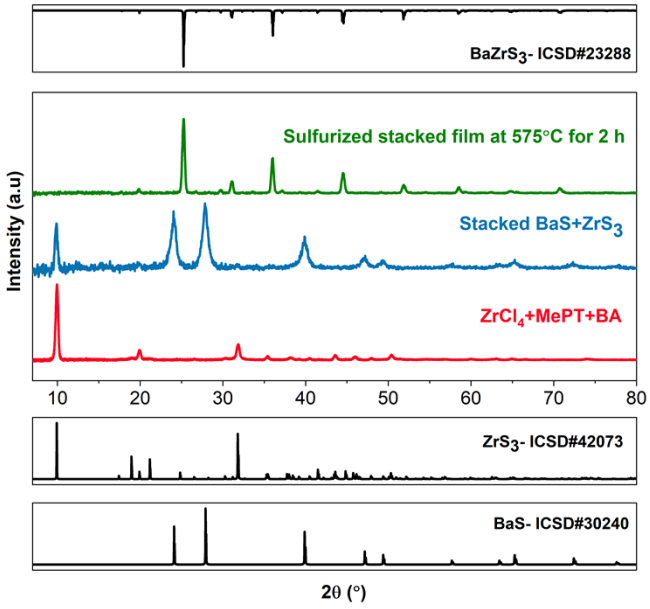

Figure S18. X-ray diffraction pattern of ZrS_3, as-coated bilayer stack of ZrS_3 and BaS, and $BaZrS_3$ after sulfurization where ZrS_3 is synthesized from $ZrCl_4$-2-methyl-2-propanethiol-butylamine solution chemistry. The stacked film was sulfurized at 575 °C for 2 h.

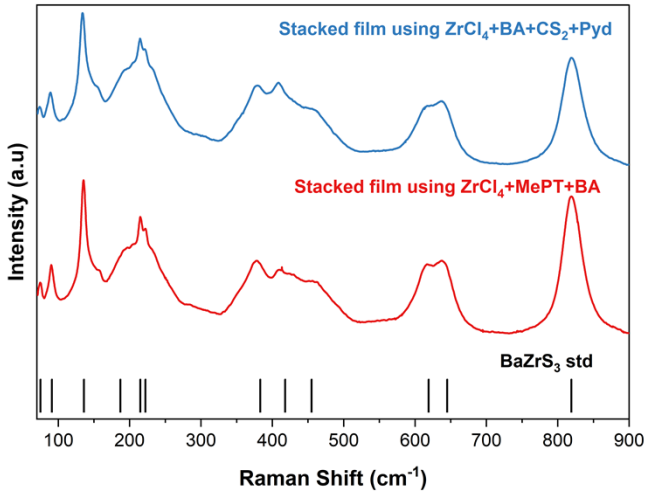

Figure S19. Raman spectra of $BaZrS_3$ films synthesized from the BaS-ZrS_3 stacked film. ZrS_3 layer was achieved through the sulfurization of as-annealed film $ZrCl_4$ solution chemistries. The films were sulfurized at 575 °C for 6 h. Reference Raman peaks were identified by Pandey et al.[1]

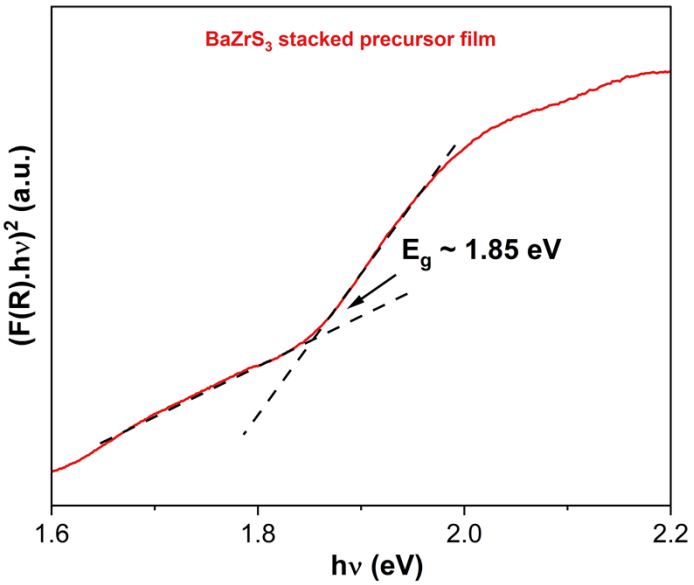

Figure S20. Kubelka-Munk transformation applied to the diffuse reflectance spectra of the $BaZrS_3$ film derived from stacked BaS-ZrS_3 precursor film. The stacked film was sulfurized at 575 °C for 2 h.

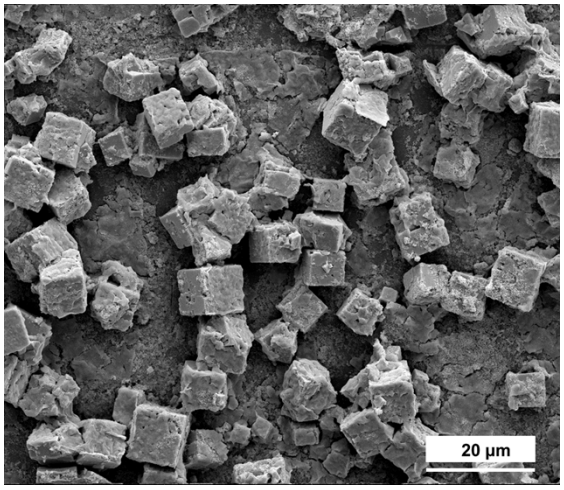

Figure S21. SEM top view of $BaZrS_3$ after sulfurization of ZrS_3-BaS stack where ZrS_3 is synthesized from $ZrCl_4$-2-methyl-2-propanethiol-butylamine. The film was sulfurized at 575 °C for 2 h.

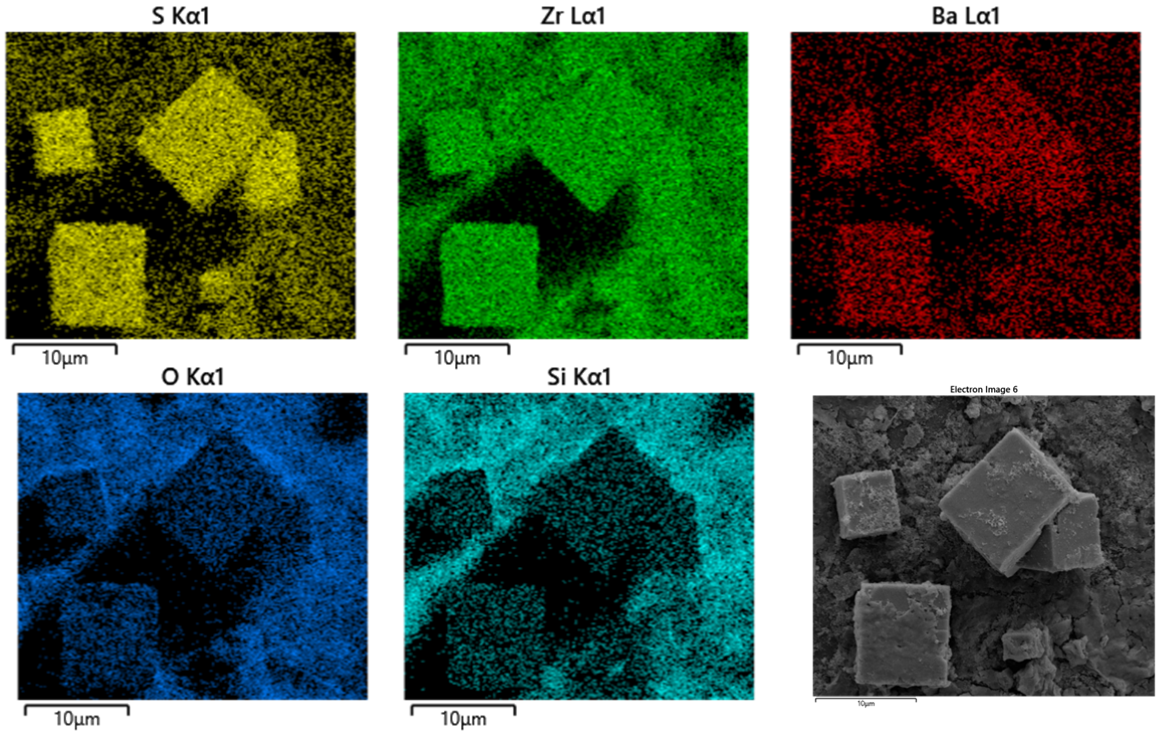

Figure S22. EDX map of $BaZrS_3$ after sulfurization of ZrS_3-BaS stack where ZrS_3 is synthesized from $ZrCl_4$-2-methyl-2-propanethiol-butylamine. The film was sulfurized at 575 °C for 2 h.

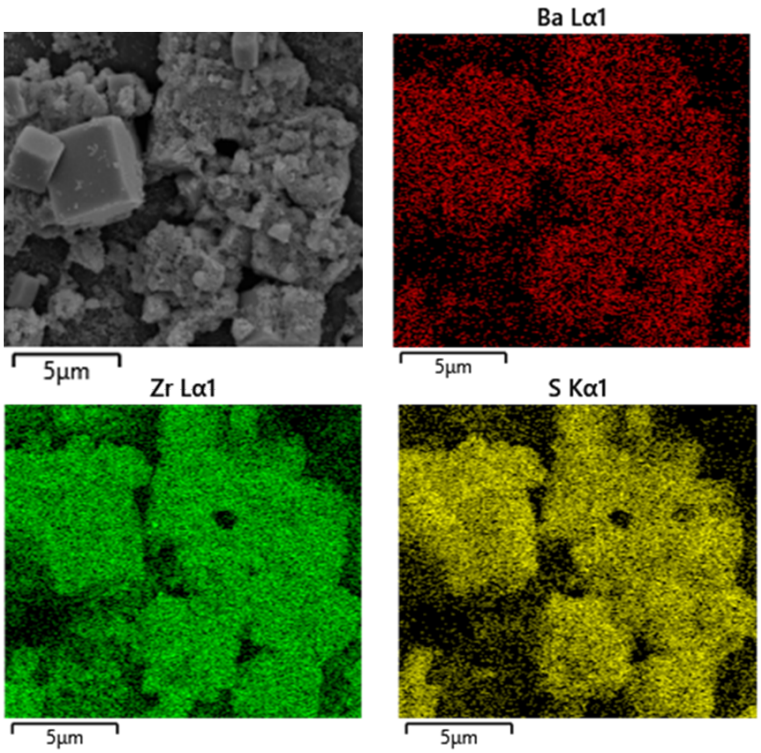

Figure S23. EDX map of $BaZrS_3$ after sulfurization of ZrS_3-BaS stack where ZrS_3 is synthesized from $ZrCl_4$-CS_2- butylamine-pyridine. The film was sulfurized at 575 °C for 2 h.

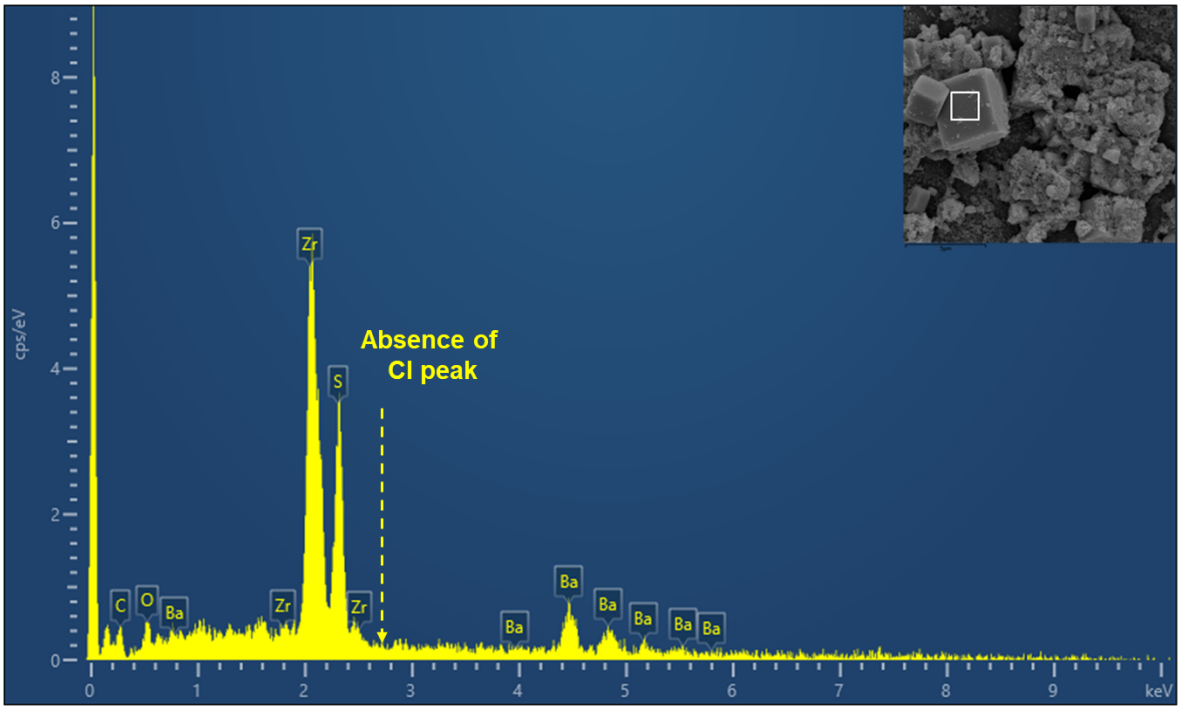

Figure S24. SEM-EDX analysis of $BaZrS_3$ after sulfurization of ZrS_3-BaS stack where ZrS_3 is synthesized from $ZrCl_4$-CS_2-butylamine-pyridine. The film was sulfurized at 575 °C for 2 h. The film does not contain any chlorine.

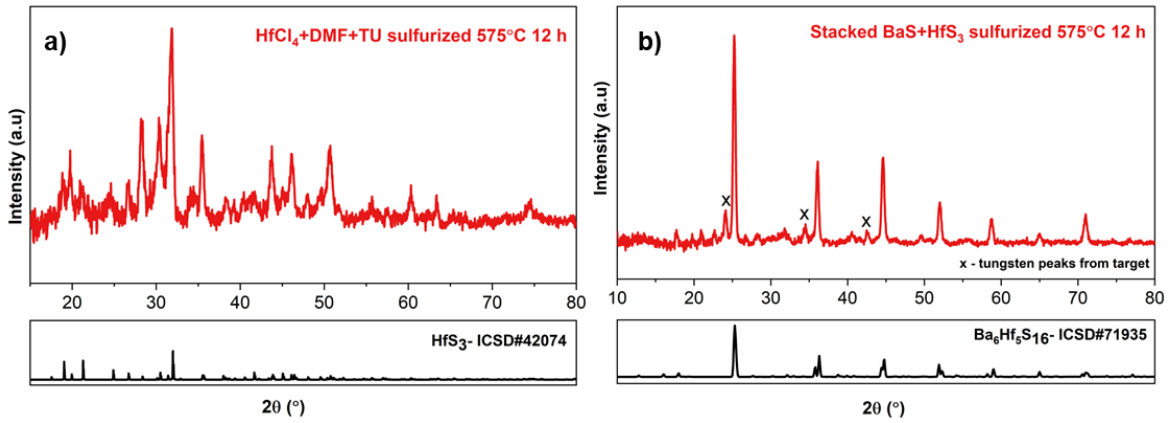

Figure S25. X-ray diffraction plot showing a) the synthesis of HfS_3 from $HfCl_4$-dimethyl formamide (DMF)-thiourea (TU) chemistry at 575 °C for 6 h and b) the synthesis of a Ruddlesden Popper phase of Ba-Hf-S synthesized from a bilayer stack of HfS_3-BaS where HfS_3 was synthesized from $HfCl_4$-dimethyl formamide-thiourea chemistry. The stacked film was sulfurized at 575 °C for 2 h.

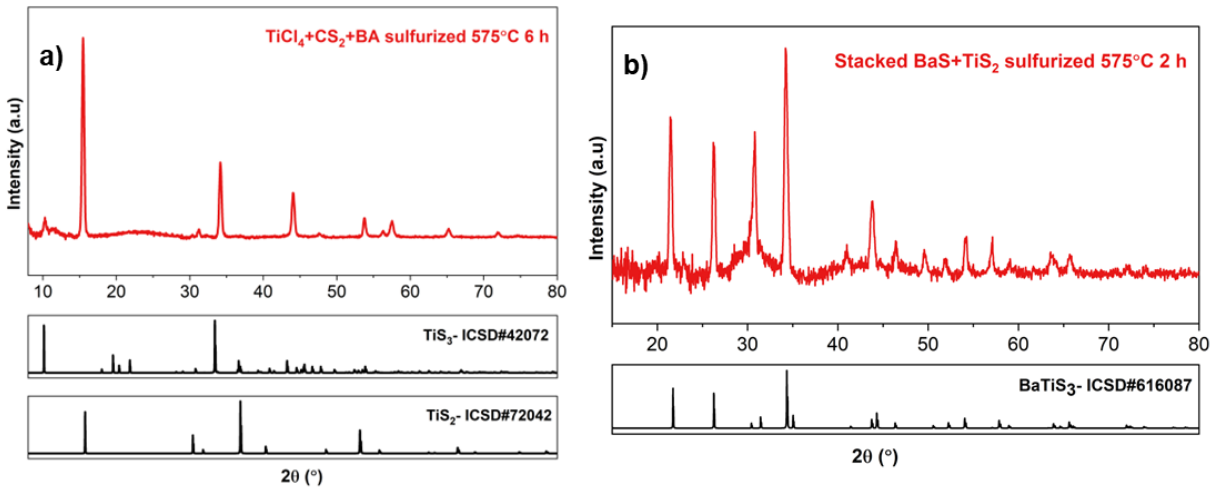

Figure S26. X-ray diffraction plot showing a) the synthesis of a mixture of TiS_3 and TiS_2 from $TiCl_4$-CS_2-butylamine (BA)-pyridine (Pyd) chemistry at 575 °C for 6 h and b) the synthesis of $BaTiS_3$ from a bilayer stack of TiS_2/TiS_3-BaS. The stacked film was sulfurized at 575 °C for 2 h.

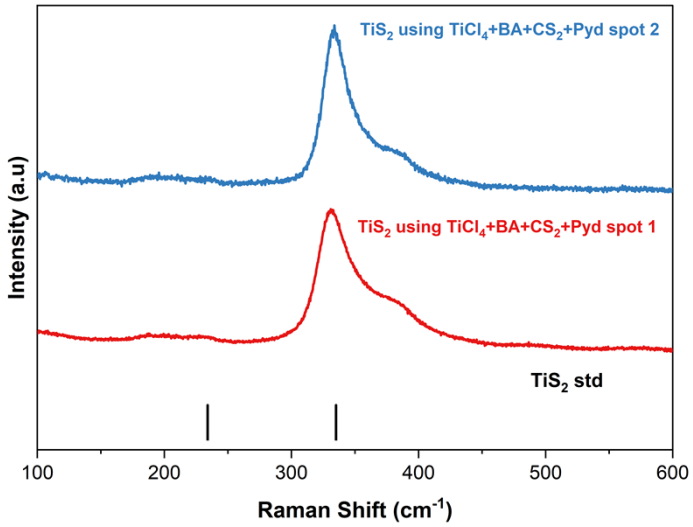

Figure S27. Raman of TiS_2 film synthesized from $TiCl_4$-butylamine (BA)-CS_2-pyridine (Pyd) and sulfurized at 575 °C for 6 h.

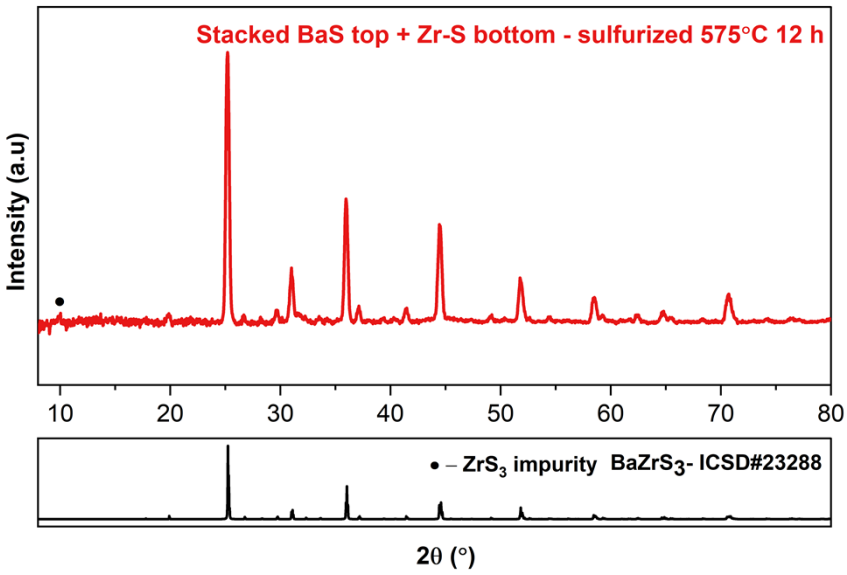

Figure S28. X-ray diffraction pattern of $BaZrS_3$ after sulfurization of as annealed ZrS_x and BaS stack where ZrS_x is synthesized from $ZrCl_4$-butylamine-CS_2-pyridine. The film was sulfurized at 575 °C for 12 h.

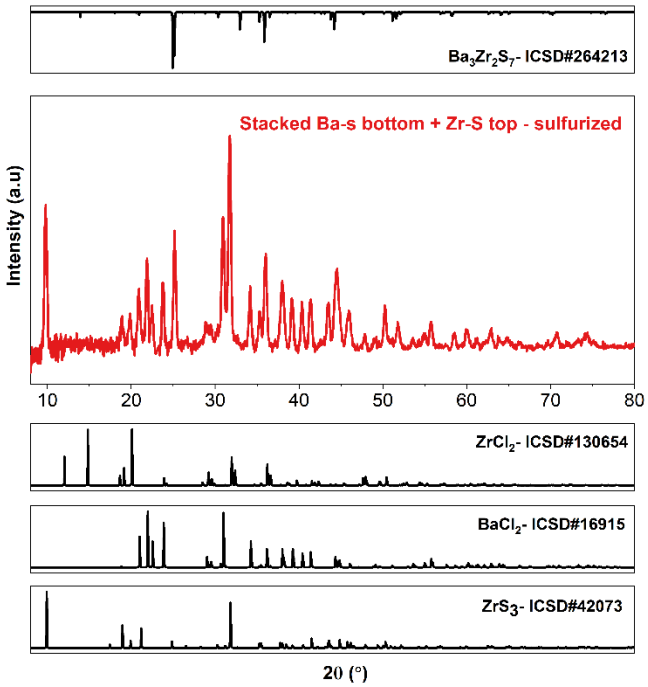

Figure S29. X-ray diffraction pattern confirmed chlorine impurity after the sulfurization of a stack of BaS at the bottom and as annealed ZrS_x at the top where ZrS_x is synthesized from $ZrCl_4$-butylamine-CS_2-pyridine. The film was sulfurized at 575 °C for 12 h and showed a secondary $BaCl_2$ phase.

Hybrid colloidal precursor

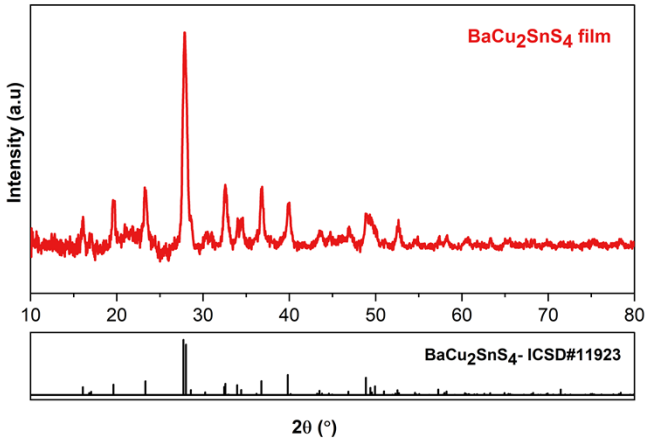

Figure S30. X-ray diffraction pattern of Cu_2BaSnS_4 synthesized from fully dissolved metal sulfides/pure metal precursor ink. Cu_2S, BaS, and Sn powder were dissolved in a mixture of propylamine-CS_2-pyridine to form a 0.4 M total metal concentration ink. The ink was dropcasted at 350 °C and annealed for 10 min.

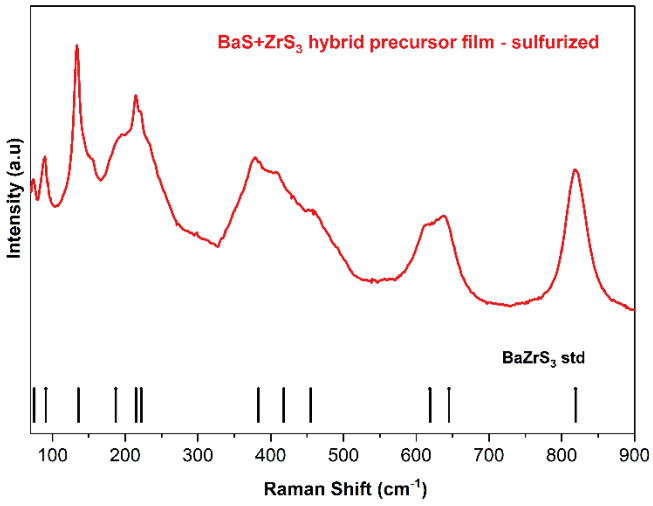

Figure S31. Raman spectra confirmed the synthesis of $BaZrS_3$ from a hybrid precursor ink of dissolved BaS and suspended ZrS_3. The film was sulfurized at 575 °C for 2 h. ZrS_3 was synthesized from sulfurization of Zr nanopowder, resulting in less than 1-micron size grains of ZrS_3. Reference Raman peaks were identified by Pandey et al.[1]

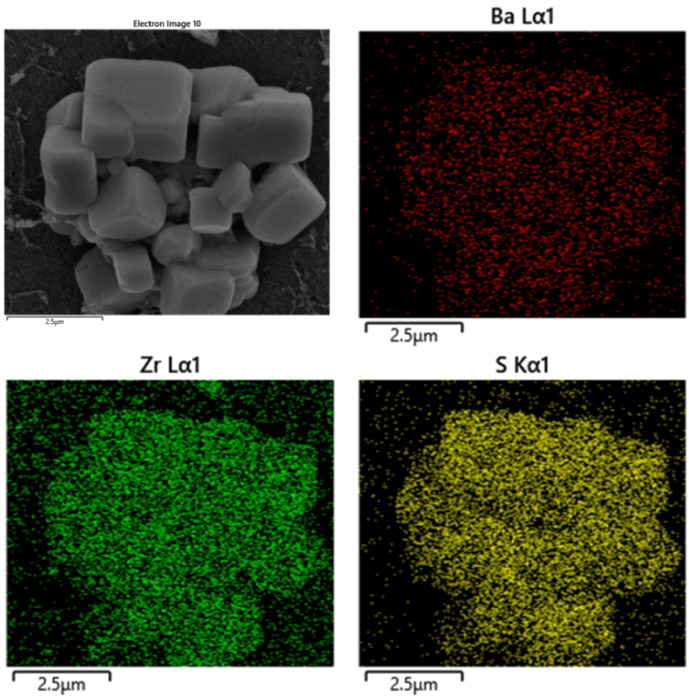

Figure S32. EDX map of $BaZrS_3$ after sulfurization of as-coated film from ZrS_3-BaS hybrid precursor ink. The film was sulfurized at 575 °C for 2 h. ZrS_3 was synthesized from the sulfurization of Zr nanopowder, resulting in less than 1-micron grains of ZrS_3.

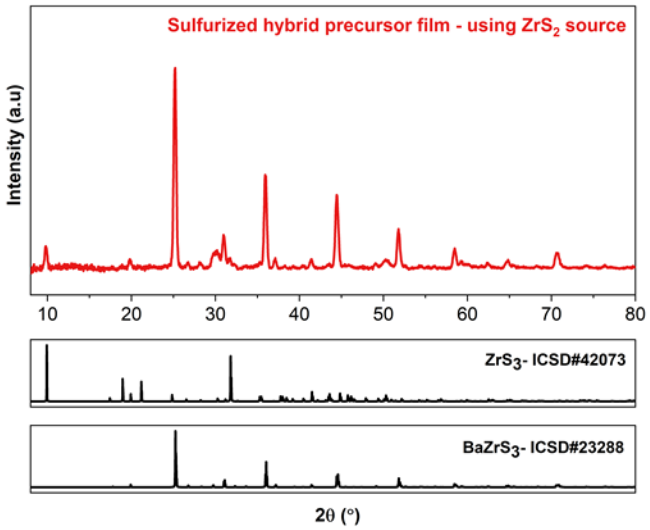

Figure S33. XRD pattern of $BaZrS_3$ after sulfurization of a doctor blade coated ZrS_3-BaS hybrid precursor ink, where ZrS_3 was synthesized from sulfurization of bulk ZrS_2 powder, resulting in large grains of ZrS_3. The film was sulfurized at 575 °C for 2 h and contains unreacted ZrS_3 and BaS_3 along with $BaZrS_3$.

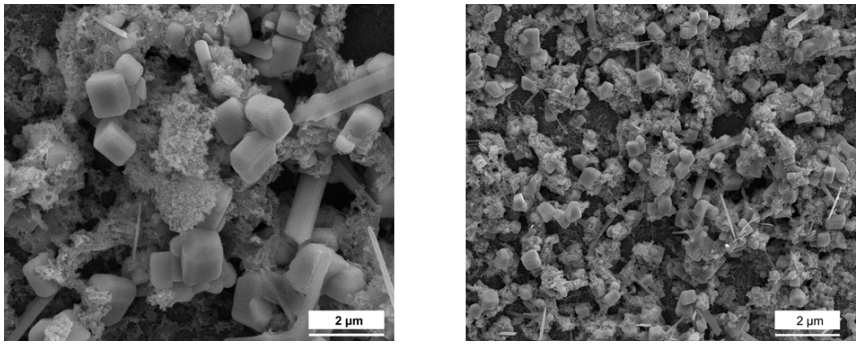

Figure S34. SEM top view of $BaZrS_3$ after sulfurization of a doctor blade coated ZrS_3-BaS hybrid precursor ink, where ZrS_3 was synthesized from sulfurization of bulk ZrS_2 powder resulting in large grains of ZrS_3. The film was sulfurized at 575 °C for 2 h and contains unreacted ZrS_3 and BaS_3 along with $BaZrS_3$.

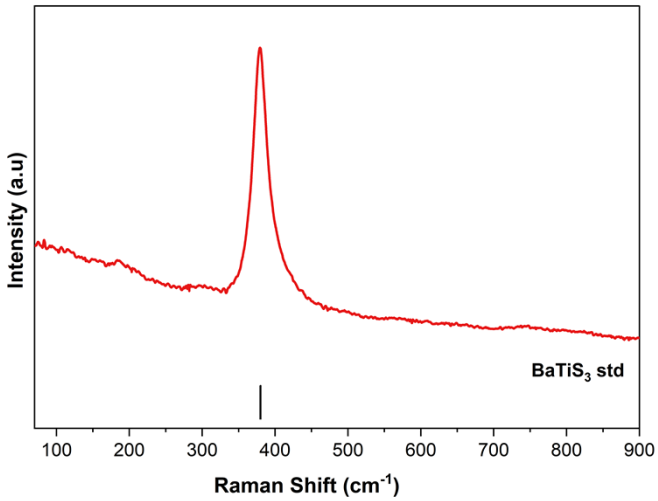

Figure S35. Raman spectra confirmed the synthesis of $BaTiS_3$ from a hybrid precursor ink of dissolved BaS and suspended TiS_2. The film was sulfurized at 575 °C for 2 h. TiS_2 was synthesized from the sulfurization of TiH_2 nanopowder.

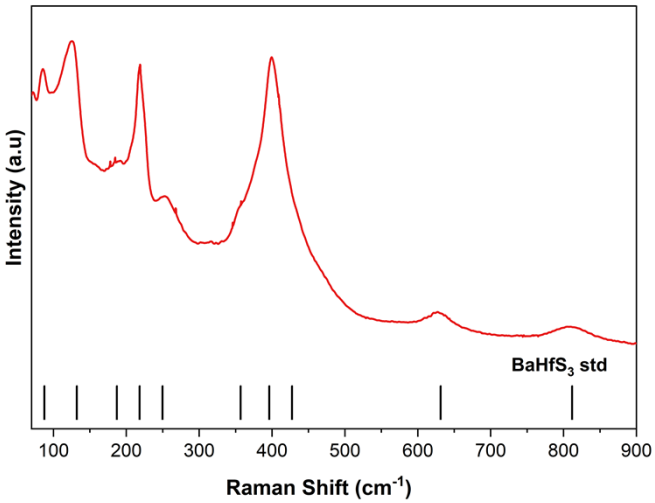

Figure S36. Raman spectra confirmed the synthesis of $BaHfS_3$ from a hybrid precursor ink of dissolved BaS and suspended HfS_3. The film was sulfurized at 575 °C for 2 h. HfS_3 was synthesized from the sulfurization of HfH_2 nanopowder.

Selenium liquid flux

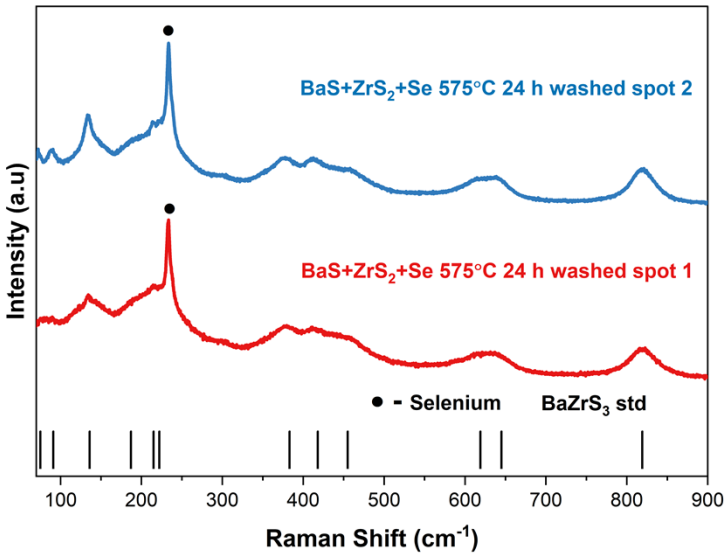

Figure S37. Raman of water-washed $BaZrS_3$ synthesized from Se flux at 575 °C for 24 h. Raman shows that slight impurities of selenium remained in the powder. However, the excess selenium can readily dissolve in an amine-thiol mixture or other solution chemistries. Reference Raman peaks were identified by Pandey et al.[1]

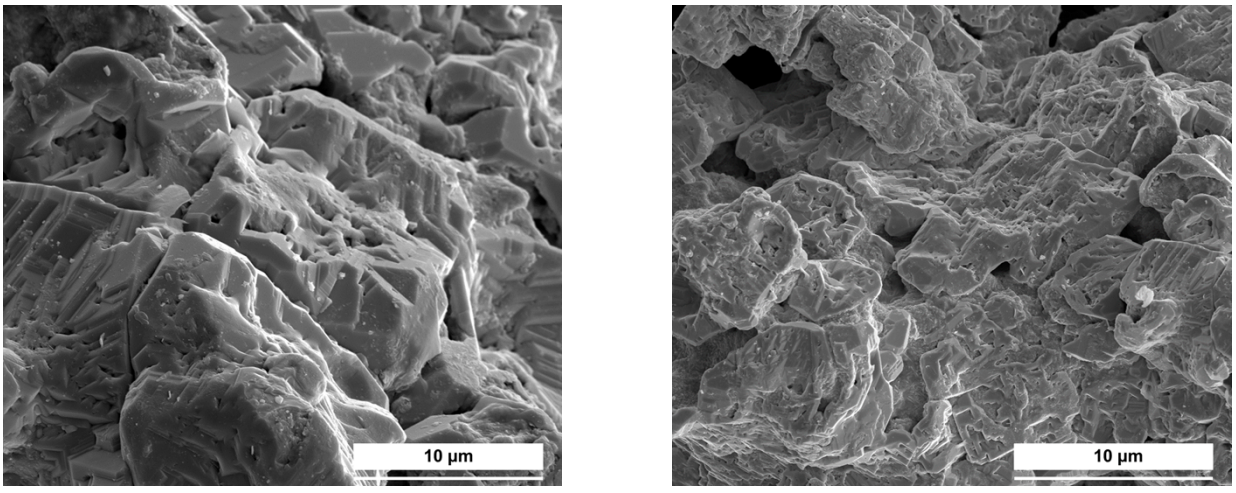

Figure S38. SEM images of water-washed $BaZrS_3$ synthesized from selenium liquid flux at 575 °C for 24 h.

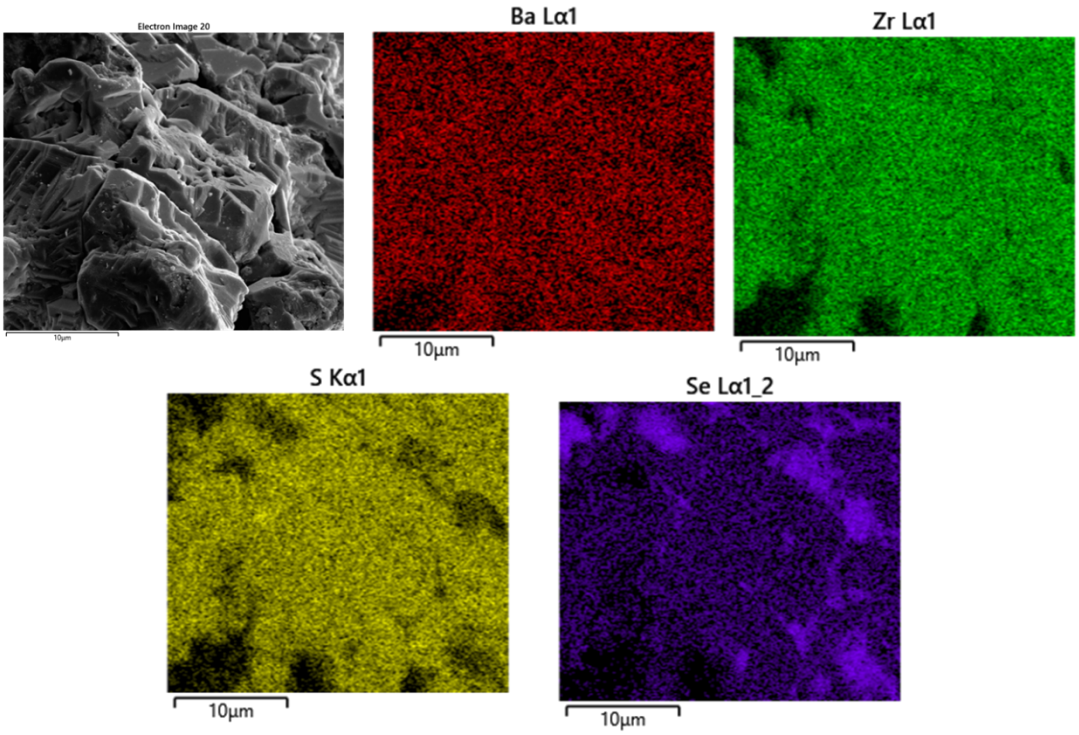

Figure S39. SEM-EDX analysis of water-washed $BaZrS_3$ synthesized from selenium liquid flux at 575 °C for 24 h. The $BaZrS_3$ grains predominantly contain Ba, Zr, and S, with negligible selenium within the grain. However, some pockets of residual bulk selenium remained, which can be removed with a relevant solution treatment.

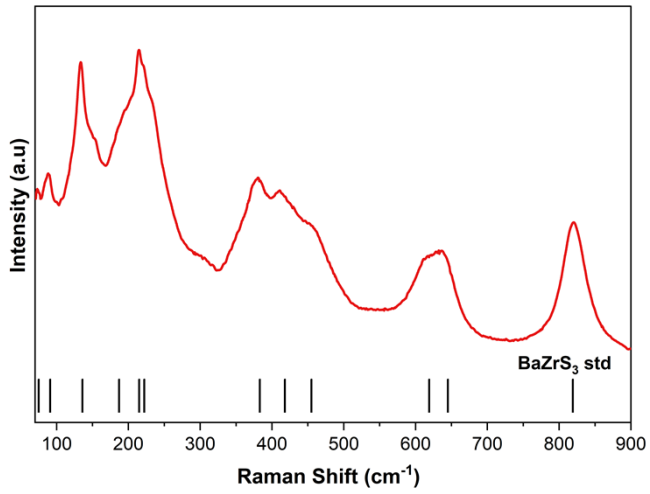

Figure S40. Raman of amine-thiol washed $BaZrS_3$ synthesized from Se flux at 575 °C for 24 h. After the water wash, the $BaZrS_3$ powder was rinsed in a propylamine-ethanedithiol mixture (5:1 vol:vol). The residual selenium was washed away. Reference Raman peaks were identified by Pandey et al.[1]

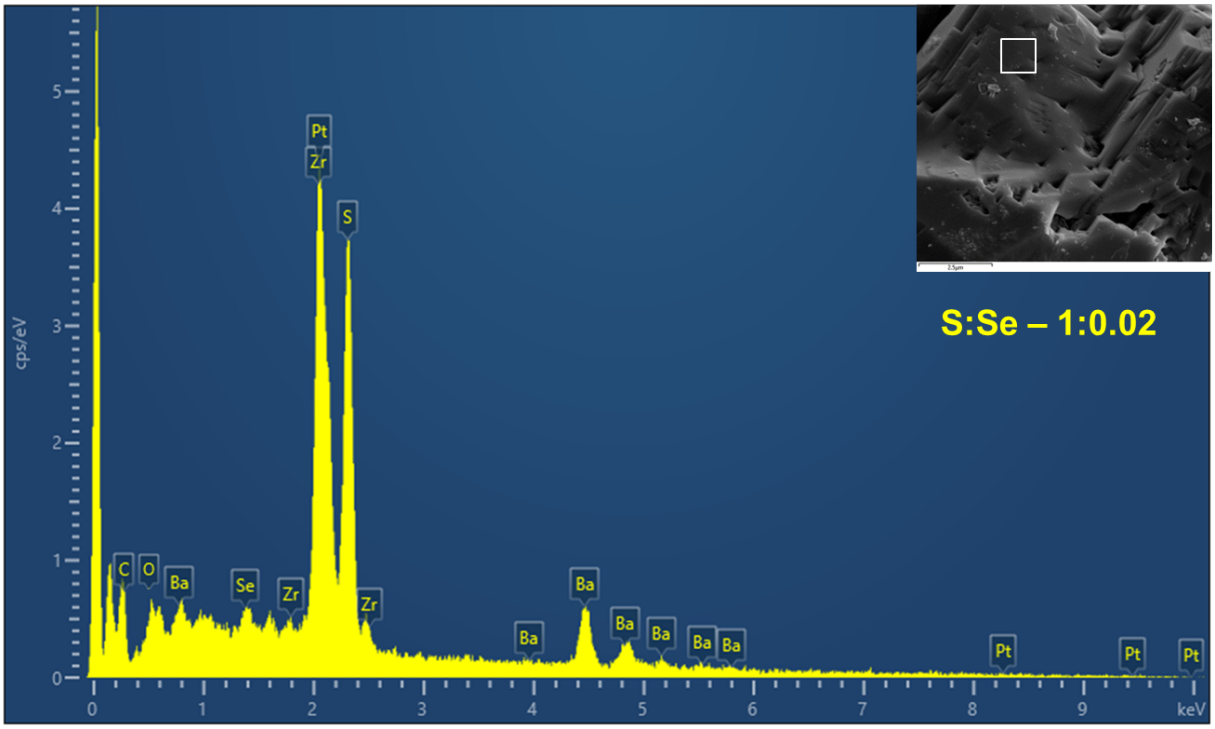

Figure S41. SEM-EDX analysis of water-washed $BaZrS_3$ synthesized from selenium liquid flux at 575 °C for 24 h. The $BaZrS_3$ grains predominantly contain Ba, Zr, and S, with negligible selenium within the grain. After the water wash, the $BaZrS_3$ powder was rinsed in a propylamine-ethanedithiol mixture (5:1 vol:vol). The residual selenium was washed away. However, the EDX analysis shows that the grains are Ba-poor. It might be because some Ba was lost as $BaSe_3$.

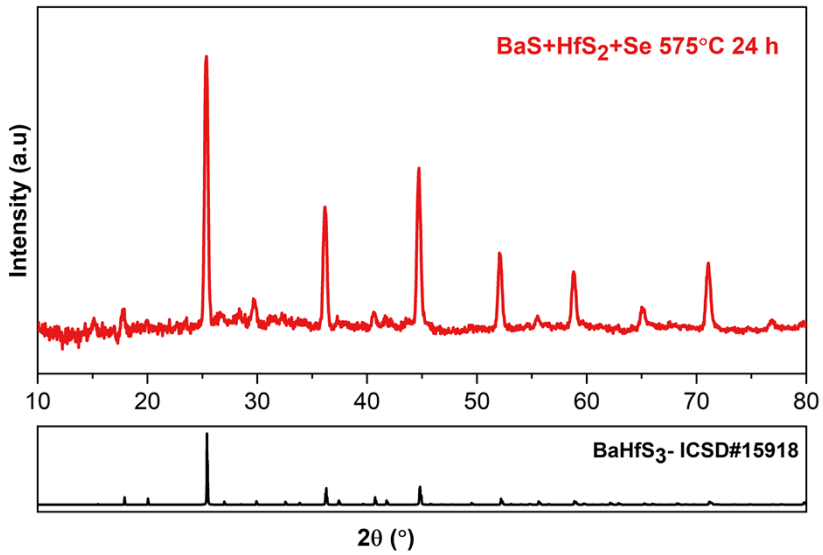

Figure S42. X-ray diffraction plot of water-washed $BHfS_3$ synthesized from selenium liquid flux at 575 °C for 2 h.

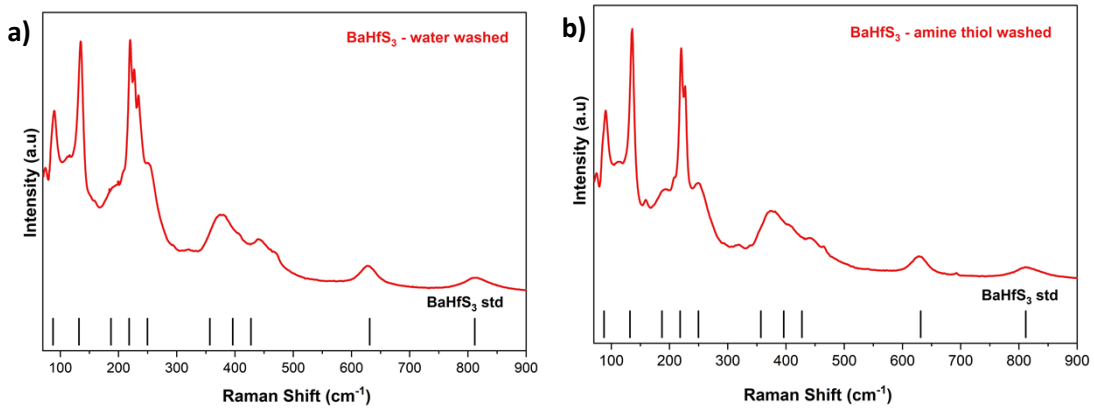

Figure S43. Raman spectra of a) water-washed $BaHfS_3$ and b) propylamine-ethanedithiol-washed $BaHfS_3$ synthesized from selenium liquid flux at 575 °C for 24 h.

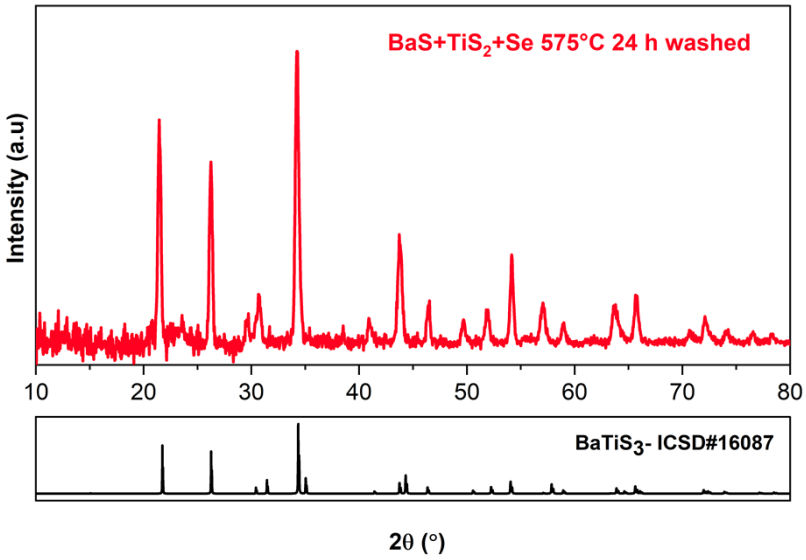

Figure S44. X-ray diffraction plot of water-washed $BaTiS_3$ synthesized from selenium liquid flux at 575 °C for 24 h.

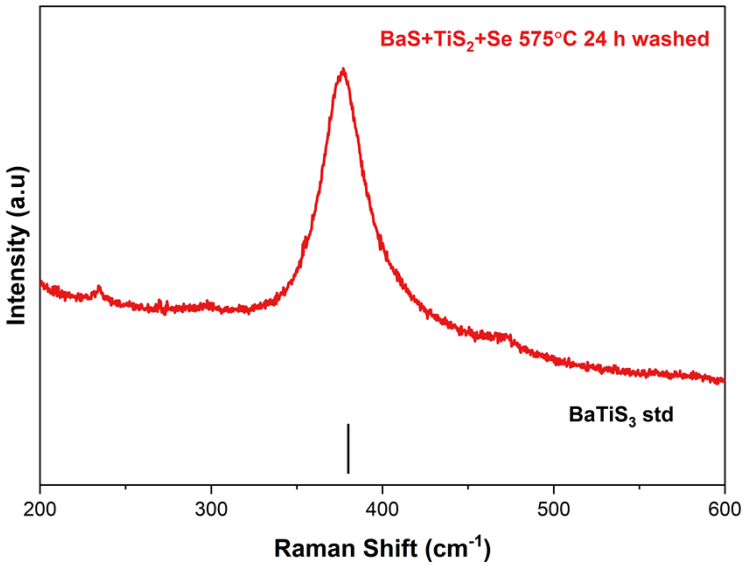

Figure S45. Raman spectra of water-washed $BaTiS_3$ synthesized from selenium liquid flux at 575 °C for 24 h.

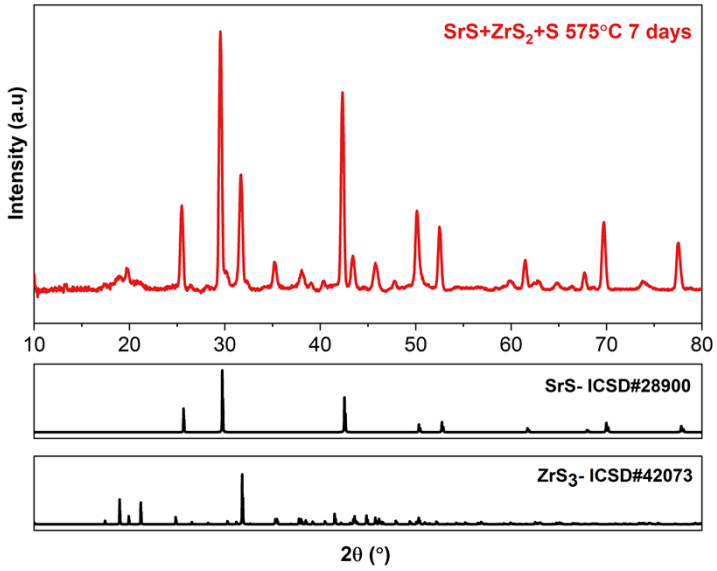

Figure S46. X-ray diffraction plot showing that the heating of the binary sulfides for the potential synthesis of $SrZrS_3$ in the presence of sulfur did not result in a ternary phase even after 7 days

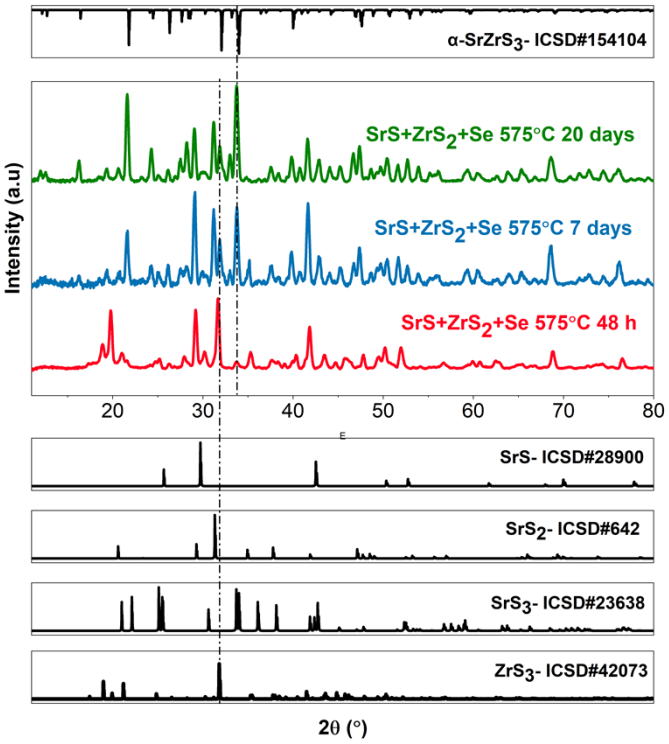

Figure S47. X-ray diffraction plot of the time evolution of α-$SrZrS_3$ phase synthesized using binary sulfides and selenium liquid flux at 575 °C.

References:

(1) Pandey, J.; Ghoshal, D.; Dey, D.; Gupta, T.; Taraphder, A.; Koratkar, N.; Soni, A. Local Ferroelectric Polarization in Antiferroelectric Chalcogenide Perovskite BaZrS3 Thin Films. *Phys Rev B* **2020**, *102* (20), 205308. https://doi.org/10.1103/PhysRevB.102.205308.

(2) Osada, K.; Bae, S.; Tanaka, M.; Raebiger, H.; Shudo, K.; Suzuki, T. Phonon Properties of Few-Layer Crystals of Quasi-One-Dimensional ZrS_3 and $ZrSe_3$. *The Journal of Physical Chemistry C* **2016**, *120* (8), 4653–4659. https://doi.org/10.1021/acs.jpcc.5b12441.